



# ME 6135: Advanced Aerodynamics

**Dr. A.B.M. Toufique Hasan**

**Professor**

**Department of Mechanical Engineering**

**Bangladesh University of Engineering & Technology (BUET), Dhaka**

## **Lecture-11**

**23/11/2024**

**Problem Classical Thin Airfoil Theory**

**Flow Over Finite Wing (3D)**

toufiquehasan.buet.ac.bd  
toufiquehasan@me.buet.ac.bd



# Problem

4.6 The NACA 4412 airfoil has a mean camber line given by

$$\frac{z}{c} = \begin{cases} 0.25 \left[ 0.8 \frac{x}{c} - \left( \frac{x}{c} \right)^2 \right] & \text{for } 0 \leq \frac{x}{c} \leq 0.4 \\ 0.111 \left[ 0.2 + 0.8 \frac{x}{c} - \left( \frac{x}{c} \right)^2 \right] & \text{for } 0.4 \leq \frac{x}{c} \leq 1 \end{cases}$$

Using thin airfoil theory, calculate

(a)  $\alpha_{L=0}$  (b)  $c_l$  when  $\alpha = 3^\circ$

4.7 For the airfoil given in Problem 4.6, calculate  $c_{m,c/4}$  and  $x_{cp}/c$  when  $\alpha = 3^\circ$ .

4.8 Compare the results of Problems 4.6 and 4.7 with experimental data for the NACA 4412 airfoil, and note the percentage difference between theory and experiment. (*Hint: A good source of experimental airfoil data is Reference 11.*)



# Wing Geometry

- The *wing span*,  $b$ , is the straight-line distance measured from wing tip to wing tip.
- The *average chord*,  $\bar{c}$ , is determined so that the product of the span and the average chord is the wing area ( $b \times \bar{c} = S$ ).
- The *aspect ratio*,  $AR$ , is the ratio of the span and the average chord.

For a general wing, the aspect ratio is defined as:

$$AR = \frac{b^2}{S}$$

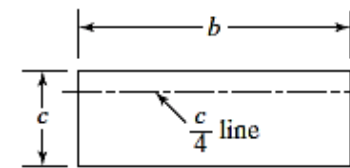
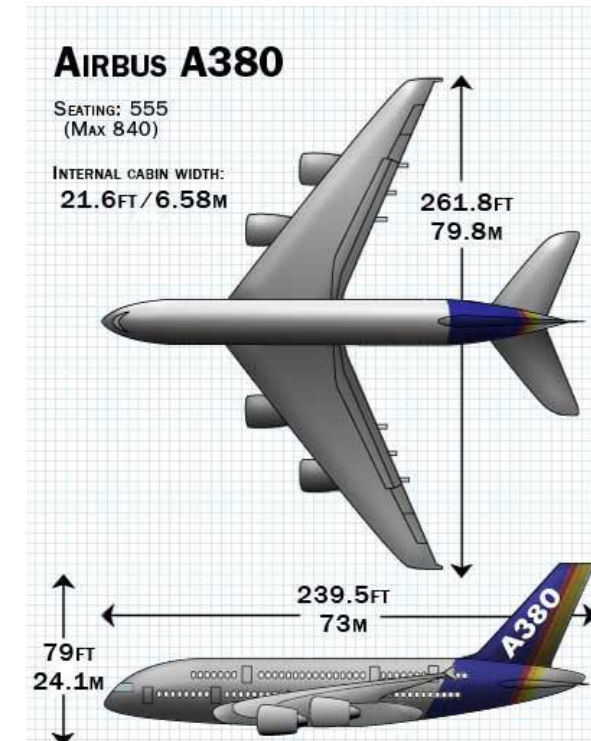
For a rectangular wing, the aspect ratio is simply:

$$AR = \frac{b}{c}$$

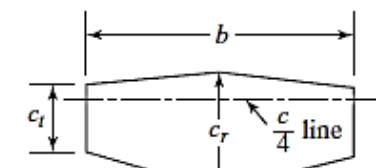
The aspect ratio is a fineness ratio of the wing and is useful in determining aerodynamic characteristics and structural weight. Typical aspect ratios vary from 35 for a high-performance sailplane to 2 for a supersonic jet fighter.

- The *root chord*,  $c_r$ , is the chord at the wing centerline, and the *tip chord*,  $c_t$ , is the chord at the wing tip.
- Considering the wing planform to have straight lines for the leading and trailing edges (half the wing will have the shape of a trapezoid), the *taper ratio*,  $\lambda$ , is the ratio of the tip chord to the root chord:

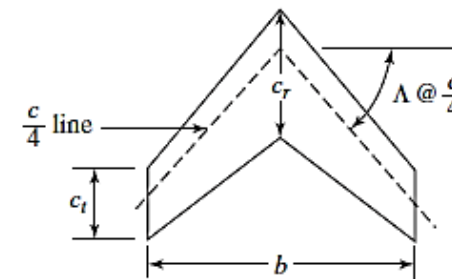
$$\lambda = \frac{c_t}{c_r}$$



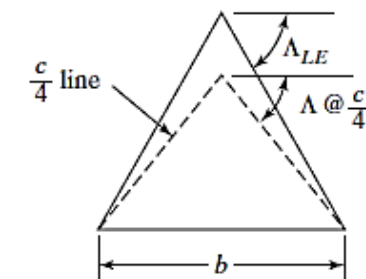
Rectangular wing



Unswept trapezoidal wing



Swept wing



Delta wing

Figure 5.7 Geometric characteristics of the wing planform.



The taper ratio affects the lift distribution and the structural weight of the wing. A rectangular wing has a taper ratio of 1.0, while a pointed tip delta wing has a taper ratio of 0.0.

- The *sweep angle*,  $\Lambda$ , is usually measured as the angle between the line of 25% chord and a perpendicular to the root chord. Sweep angles of the leading edge or of the trailing edge are also used often, since they are of interest for many applications. The sweep of a wing causes definite changes in the maximum lift, in the stall characteristics, and in the effects of compressibility.
- The *mean aerodynamic chord*,  $mac$ , is used together with  $S$  to nondimensionalize the pitch moment. Therefore, the mean aerodynamic chord represents another average chord which, when multiplied by the product of the average section moment coefficient, the dynamic pressure, and the wing area, gives the moment for the entire wing. The  $mac$  is also used to estimate the Reynolds number of the wing for skin-friction calculations. The mean aerodynamic chord is defined by:

$$mac = \frac{1}{S} \int_{-b/2}^{+b/2} [c(y)]^2 dy$$

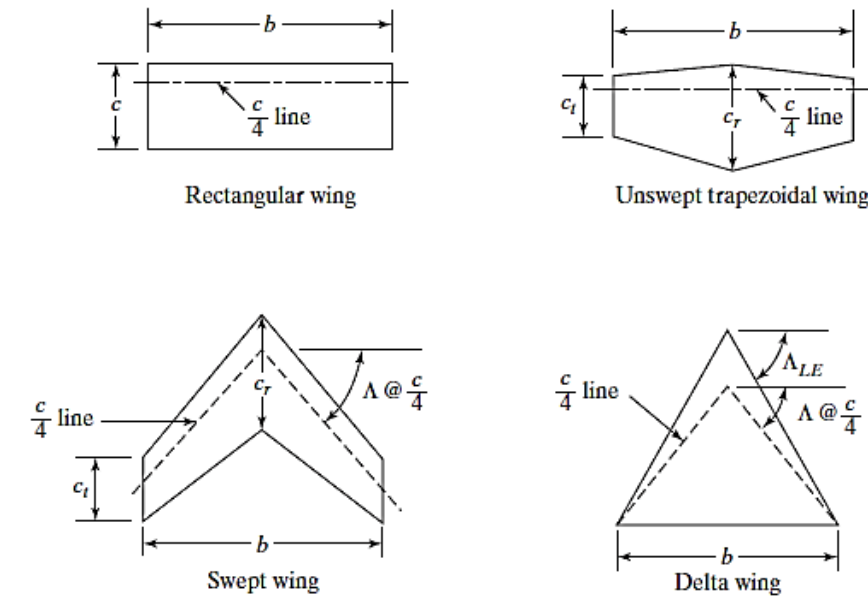


Figure 5.7 Geometric characteristics of the wing planform.







winglet

C-17 with wing flaps and leading-edge devices extended and winglets visible (U.S. Air Force photo by Abner Guzman)

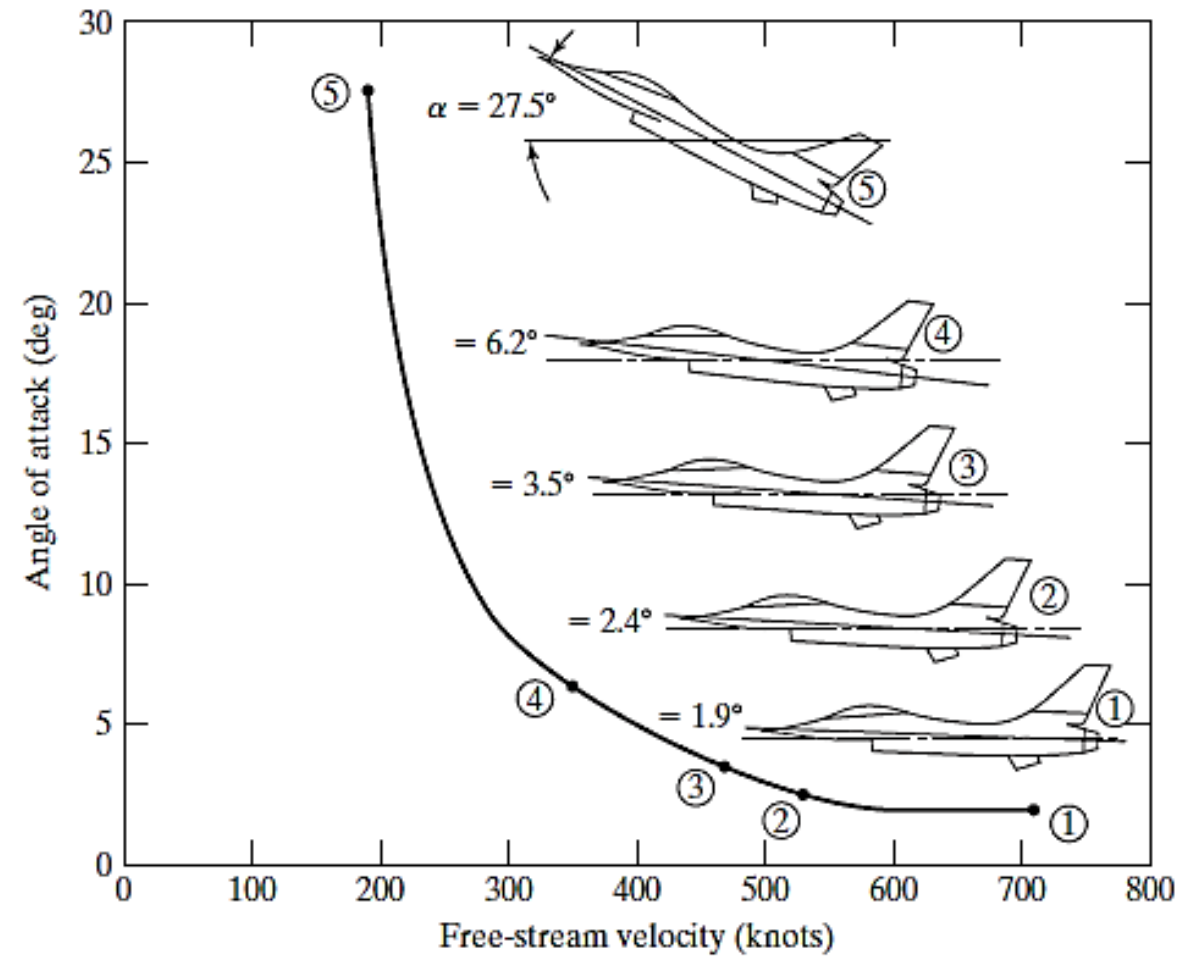


**Figure 5.28** Correlation between the angle of attack and the velocity to maintain an F-16C in steady, level, unaccelerated flight.



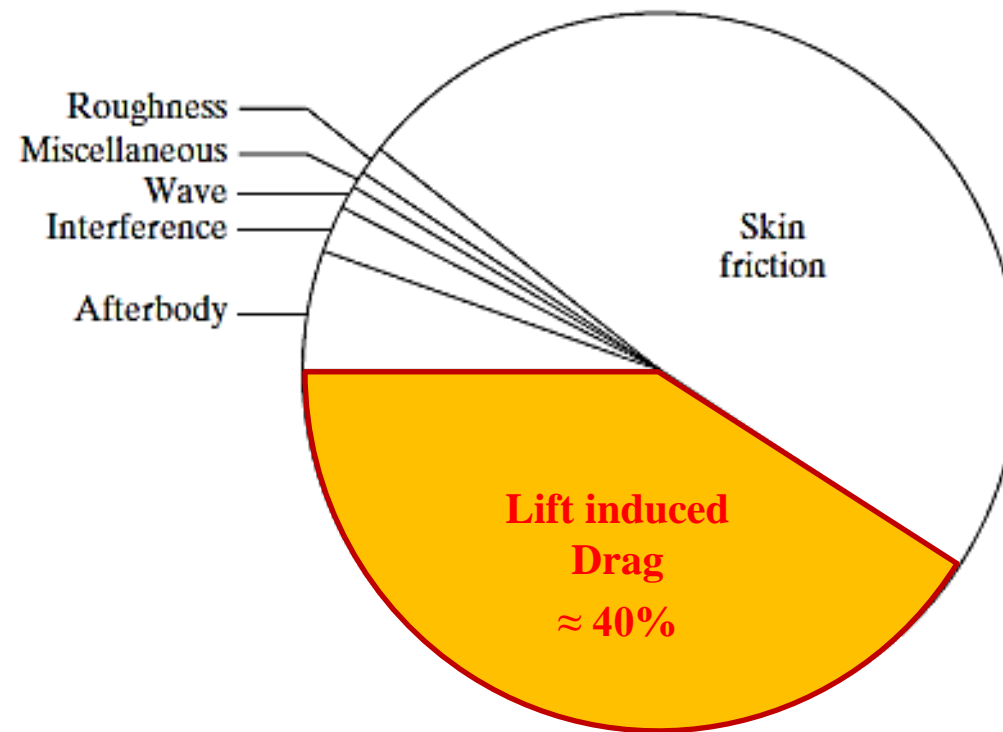
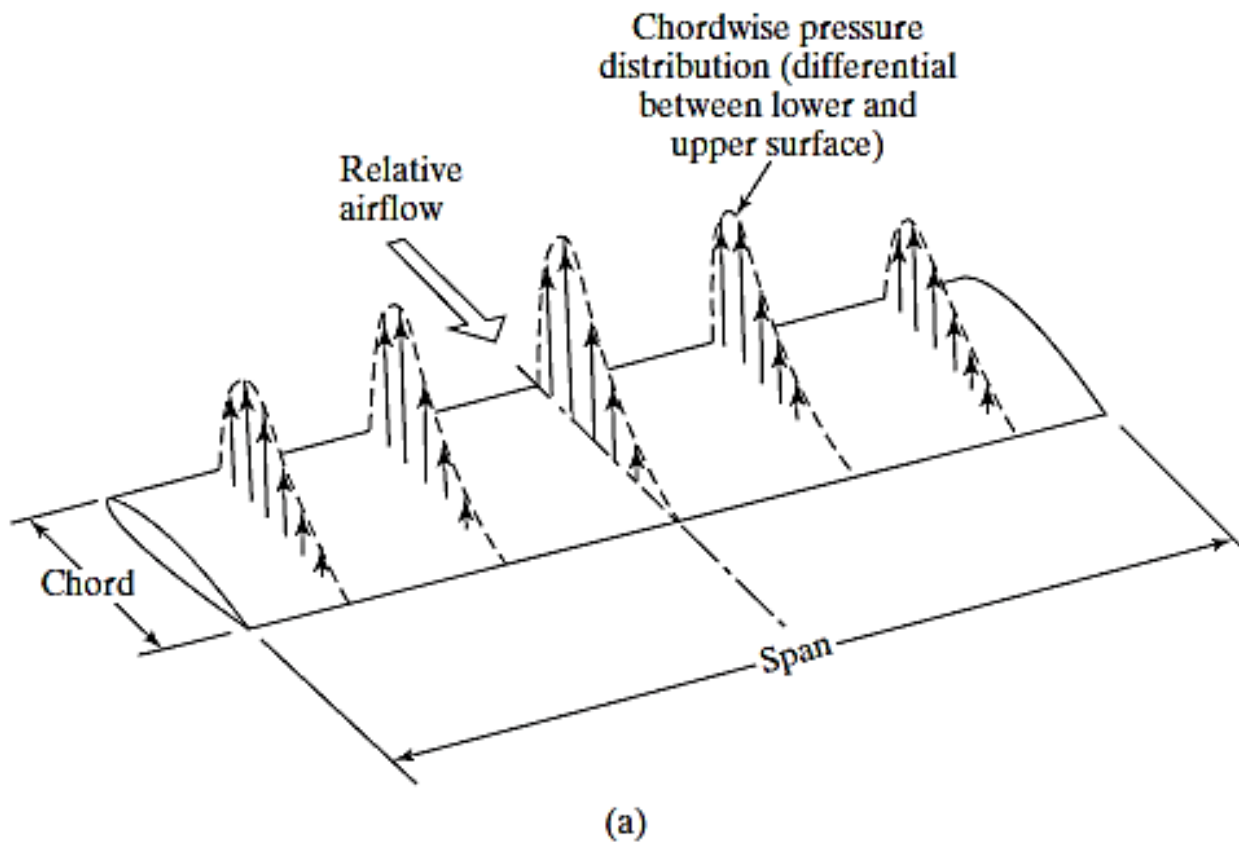
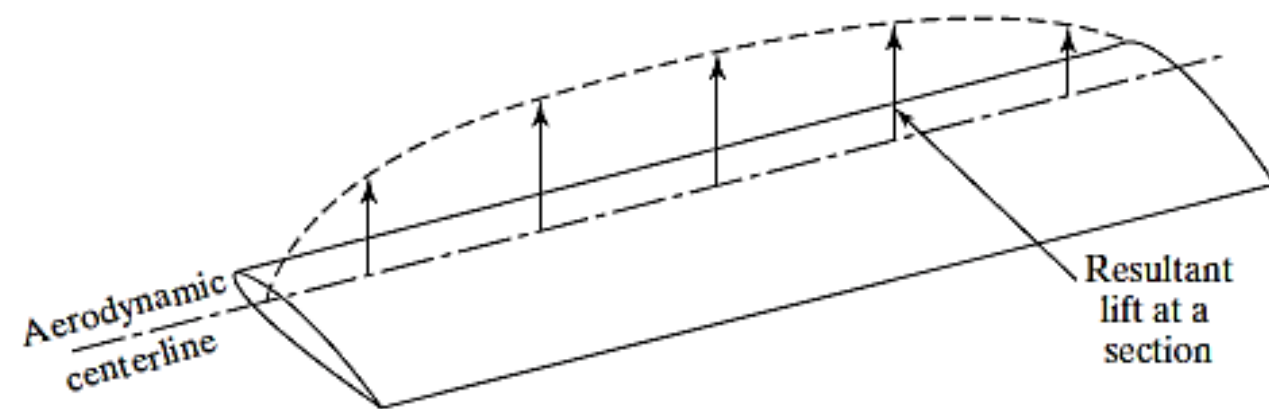


**Figure 5.30** Contributions of different drag sources for a typical transport aircraft [from Thomas (1985)]. **Sub-sonic flow**





(a)



(b)

**Figure 7.1** Aerodynamic load distribution for a rectangular wing in subsonic airstream: (a) differential pressure distribution along the chord for several spanwise stations; (b) spanwise lift distribution.





**Figure 7.3** Condensation marks the wing-tip vortices of the Space Shuttle Orbiter *Columbia* (photo courtesy NASA).



**Figure 7.4** (Continued) (b) Streamwise vorticity shedding along the trailing edge of a Boeing 747 rolling up into wing-tip vortices (courtesy of NASA Dryden Flight Research Center).





# Induced drag



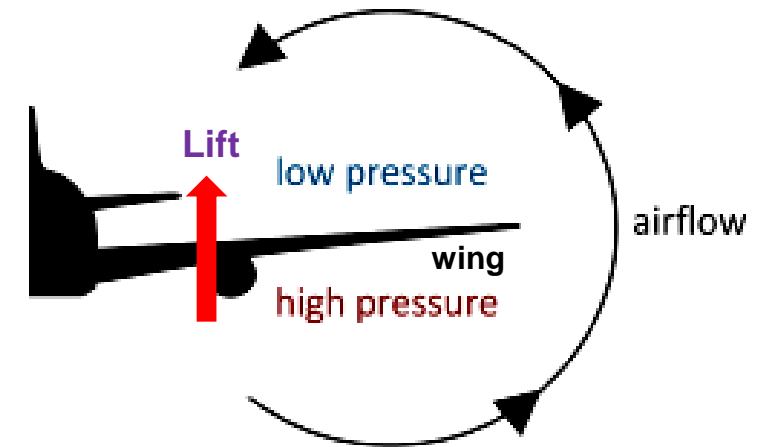
## Flow over Finite wings

An airfoil is simply a section of a wing, it might be expected that the wing to behave exactly the same as the airfoil (**?!!**).

However, the flow over an airfoil is two-dimensional (2D). In contrast, a finite wing is a three-dimensional body, and consequently the flow over the wing is three-dimensional (3D); that is, there is a component of flow in the spanwise direction.

In case of a wing, additional velocity component along the spanwise direction influences the aerodynamic performance of the wing of the aircraft.

Additional physical phenomena comes to play role on the aerodynamics of a wing.



**Spanwise velocity component around a wing**  
The aircraft is moving perpendicular outward to the slide



# Flow over Finite wings

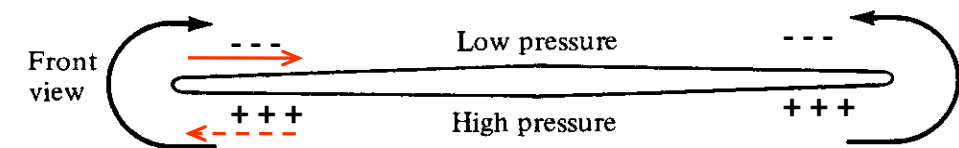
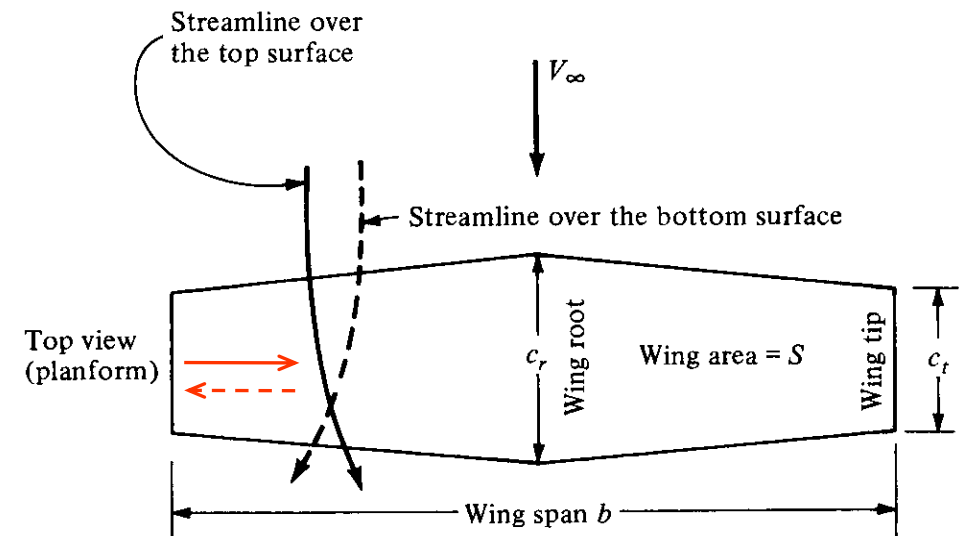
The physical mechanism for generating lift on the wing is the existence of high pressure on the bottom surface and a low pressure on the top surface.

**As a by-product of this pressure imbalance, the flow near the wing tips tends to curl around the tips**, being forced from the high-pressure region just underneath the tips to the low-pressure region on top as shown in figure.

As a result, on the wing top surface, there is generally a spanwise component of flow **from the tip toward the wing root**, causing the **streamlines over the top surface to bend toward the root**.

Similarly, on the bottom surface, there is generally a spanwise component of flow from the **root toward the tip**, causing the **streamlines over the bottom surface to bend toward the tip**.

It might seem that the flow is to “**leak**” around the wing tips.



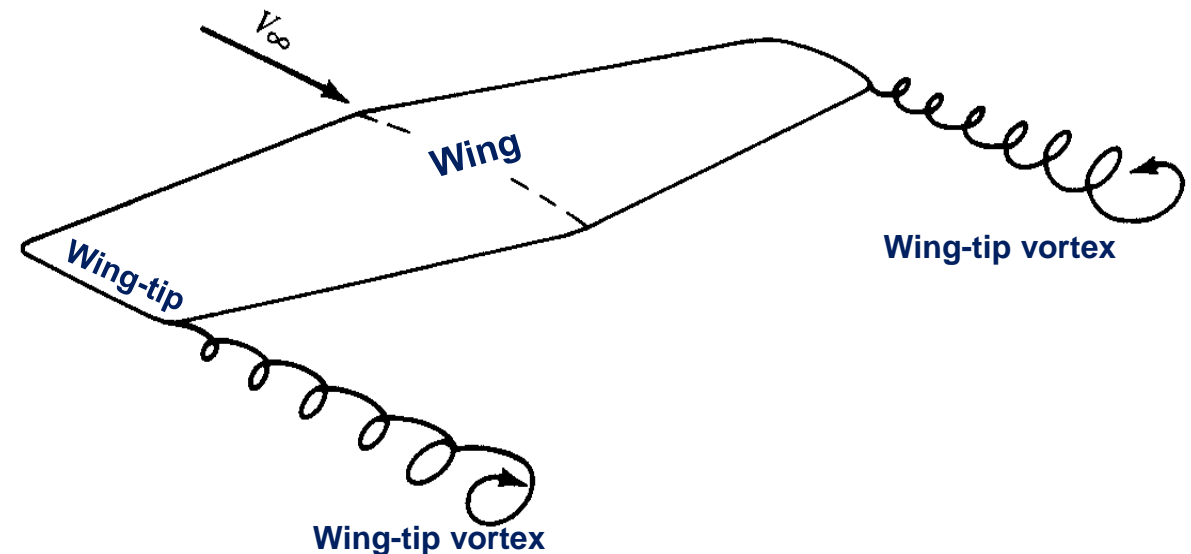
## Flow over Finite wings

This flow establishes a **circulatory motion** that trails downstream of the wing; that is, a trailing **vortex** is created at each wing tip. These are known as “**wing-tip vortices**”.

The wing-tip vortices are essentially weak “tornadoes” that trail downstream of finite wing. **These wing-tip vortices downstream of the wing induce a small downward component of air velocity in the neighborhood of the wing itself.**

Then the two vortices tend to drag the surrounding air around with them, and this secondary movement induces a small velocity component in the downward direction at the wing.

This downward component is called **downwash**, denoted by the symbol,  $w$ .



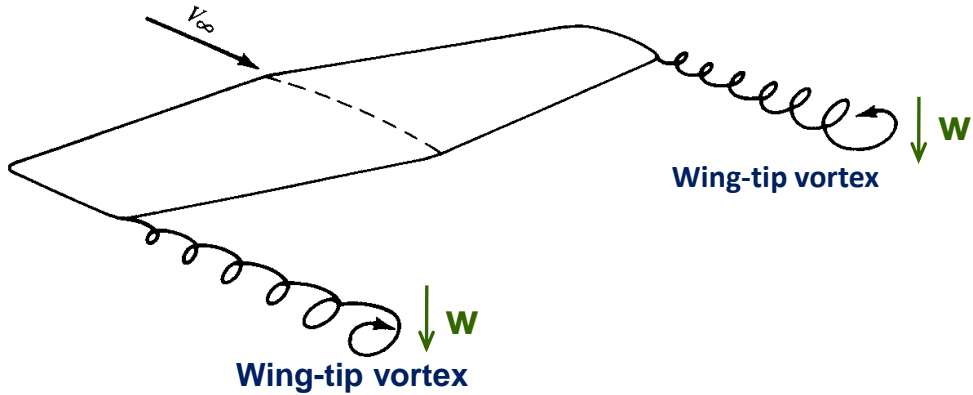
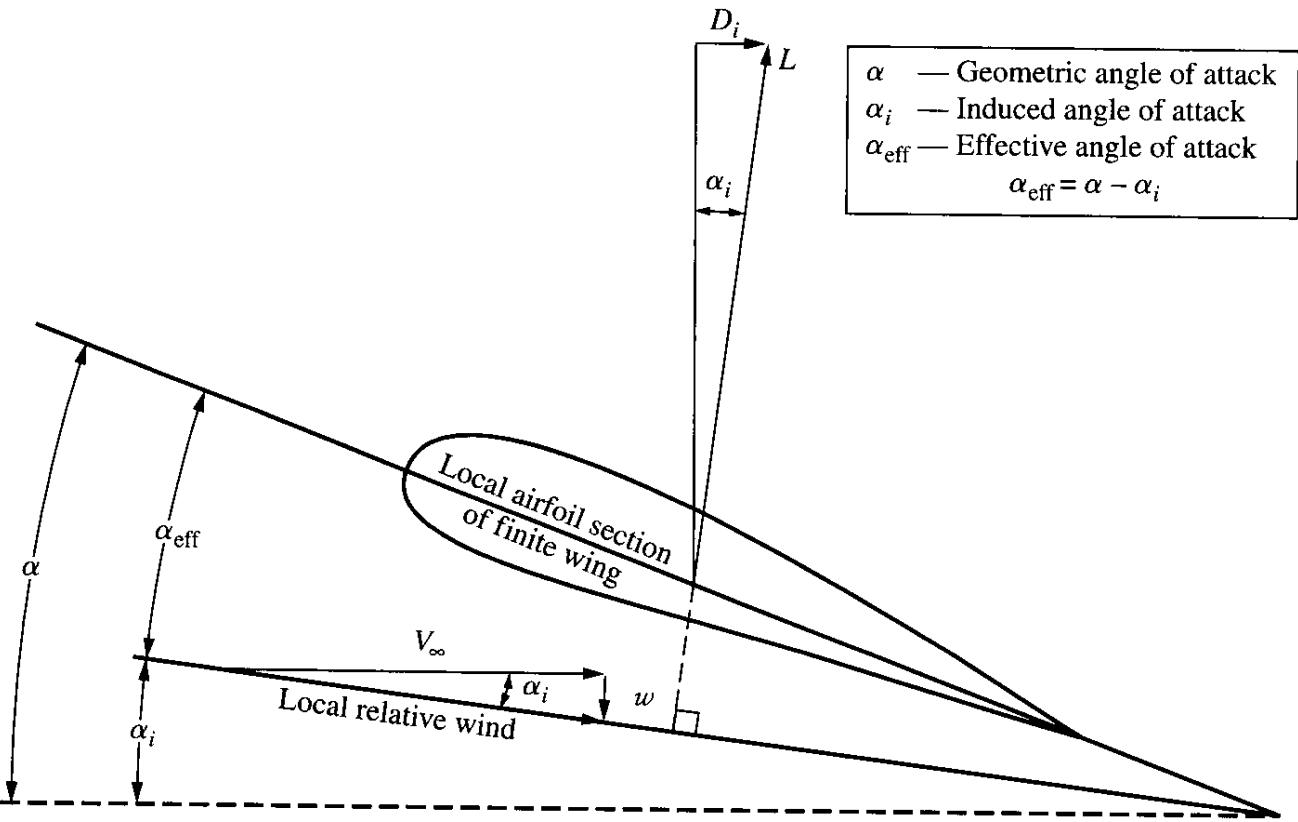
# Wing tip vortices





# Flow over Finite wings

In turn, the downwash combines with the freestream velocity  $V_\infty$  to produce a **local relative wind** which is canted downward in the vicinity of each airfoil section of the wing.



# Flow over Finite wings

The angle between the chord line and the direction of freestream is earlier defined by the angle of attack (AOA). More precisely, in case of finite wing, this angle is called as “**geometric angle of attack**”,  $\alpha$ .

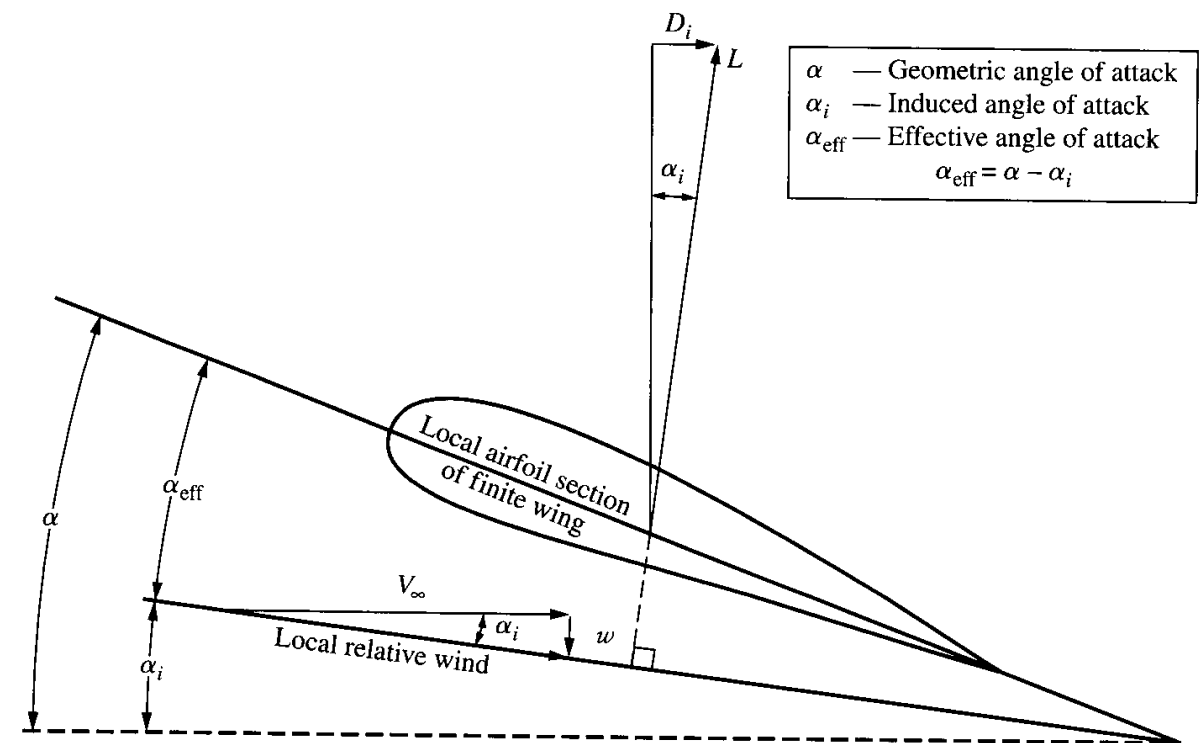
However, the **local relative wind** is inclined below the direction of  $V_\infty$  by the angle,  $\alpha_i$  which is called the **induced angle of attack**.

Two important effects are:

1. The angle of attack (AOA) actually seen by the local airfoil section is the angle between the chord line and the local relative wind, which is defined as **effective angle of attack**:

$$\alpha_{eff} = \alpha - \alpha_i$$

2. The local lift vector is aligned perpendicular to the local relative wind and is inclined behind the vertical by  $\alpha_i$ . The component of local lift vector in the freestream direction is known as **induced drag**. This is due to downwash effect in finite wing.

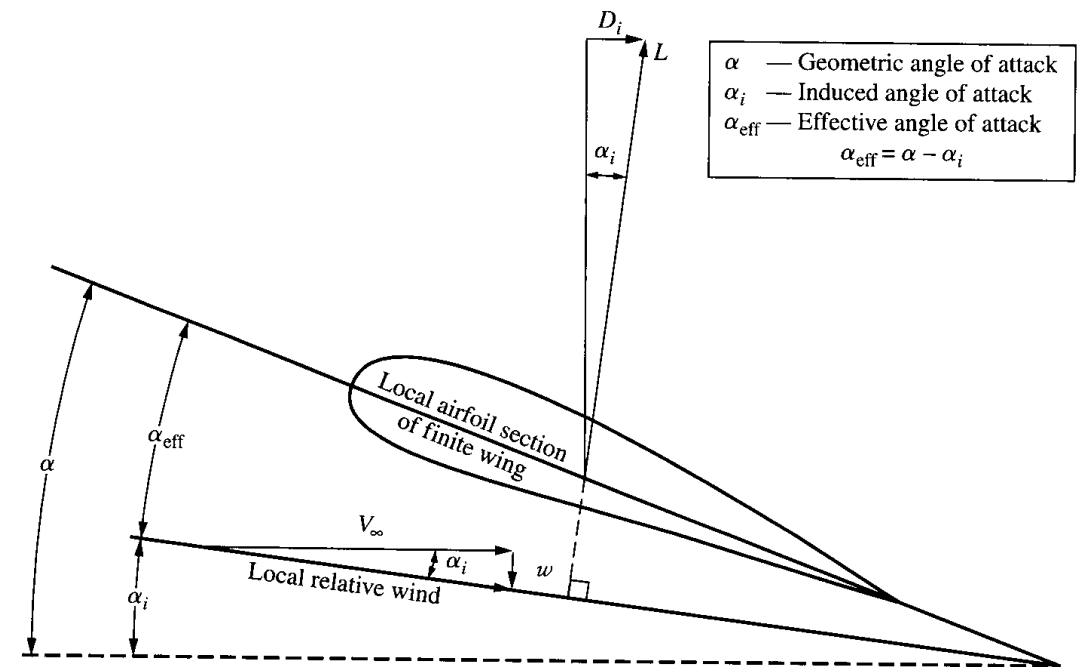


# Flow over Finite wings

In case of finite wing, a force component in the direction of freestream (**induced drag**) is found though the **inviscid, incompressible flow is still considered**. There is no relation of fluid viscosity (skin friction, viscous effect) with this type of drag.

The generation of induced drag can physically be explained as:

1. The 3-D flow induced by the wing-tip vortices alter the pressure distribution on the finite wing in such a fashion that a net pressure imbalance exists in the freestream direction. In this sense, **induced drag** is a type of “**pressure drag**”.
2. The wing tip vortices contain a large amount of translational and rotational kinetic energy. This energy has to come from somewhere; indeed, it is ultimately provided by the aircraft engine. Since, the energy of the vortices serves no useful purpose, this power is essentially lost. In fact, the extra power provided by the engine that goes into the vortices is the extra power required from the engine to overcome the induced drag.



# Flow over Finite wings

The **total drag on a subsonic finite wing in real life** is the sum of the induced drag  $D_i$ , the skin friction drag,  $D_f$ , and the pressure drag  $D_p$ . **The later two contributions are due to viscous effects.** The sum of these two viscous-dominated drag contributions is called the **profile drag**. Definition of profile drag coefficient is-

$$c_d|_{\text{profile}} = \frac{D_f + D_p}{q_\infty S}$$

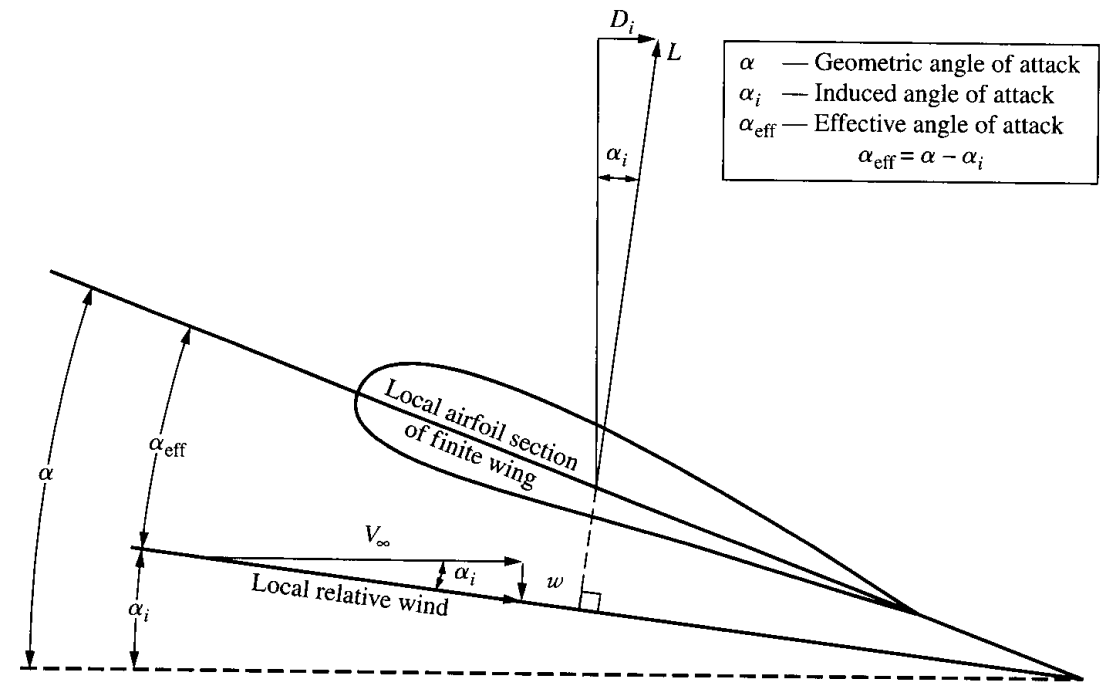
And the induced drag coefficient is-

$$C_{D,i} = \frac{D_i}{q_\infty S}$$

The **total drag coefficient** for the finite wing is-

$$C_D = c_d + C_{D,i}$$

↑
↑  
 Viscous drag      **Non-viscous drag**  
                          **Drag due to Lift**  
                          **Induced drag**



## Flow over Finite wings

**Induced drag/ Drag due to lift** can be expressed from the force triangle:

$$D_i = L \sin \alpha_i$$
$$\Rightarrow D_i \approx L \alpha_i \quad ; \alpha_i \text{ is generally small}$$

For all wings in general, the **induced angle of attack** can be found from the concept of lifting line theory and for elliptical lift distribution; the expression is written as

$$\alpha_i = \frac{C_L}{\pi e AR}$$

where  $e$  = span efficiency factor (subsonic :  $0.95 < e < 0.85$ )

$$AR = \text{Aspect ratio of the wing} = \frac{\text{span}}{\text{average chord}}$$





# Flow over Finite wings

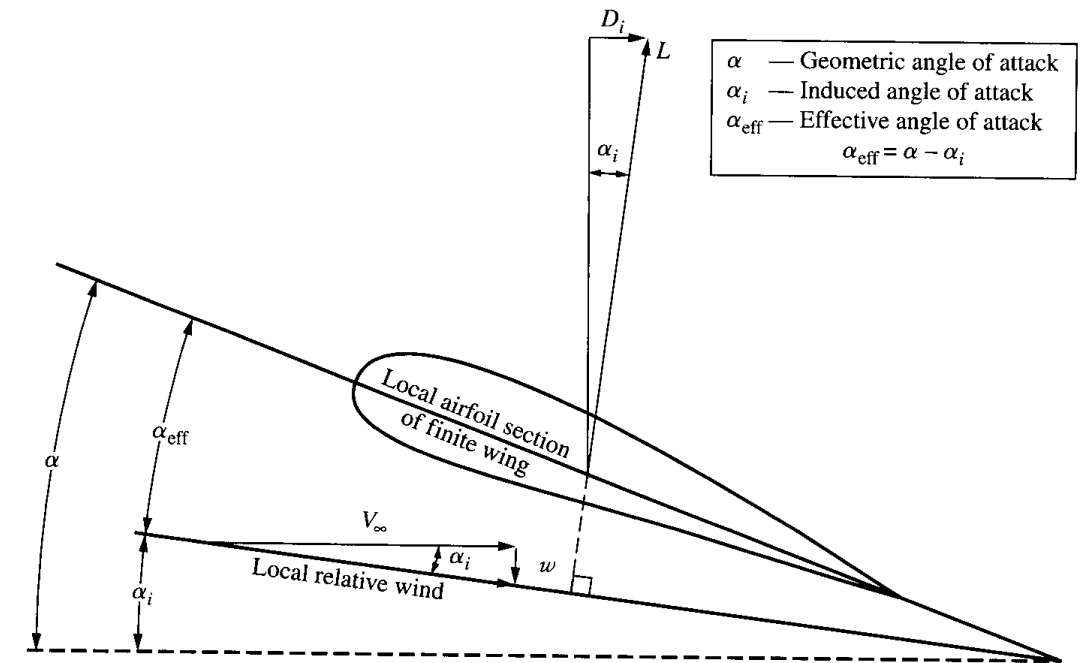
Thus the **induced drag** can be expressed as

$$D_i = L \alpha_i$$

$$\Rightarrow D_i = L \left( \frac{C_L}{\pi e AR} \right) = (q_\infty S C_L) \left( \frac{C_L}{\pi e AR} \right)$$

$$\Rightarrow \frac{D_i}{q_\infty S} = \frac{C_L^2}{\pi e AR}$$

$$\Rightarrow C_{D,i} = \frac{C_L^2}{\pi e AR}$$



# THE VORTEX FILAMENT, THE BIOT-SAVART LAW

In general, a vortex filament can be *curved*, as shown in Figure 5.8. Here, only a portion of the filament is illustrated. The filament induces a flow field in the surrounding space. If the circulation is taken about any path enclosing the filament, a constant value  $\Gamma$  is obtained. Hence, the strength of the vortex filament is defined as  $\Gamma$ . Consider a directed segment of the filament  $d\mathbf{l}$ , as shown in Figure 5.8. The radius vector from  $d\mathbf{l}$  to an arbitrary point  $P$  in space is  $\mathbf{r}$ . The segment  $d\mathbf{l}$  induces a velocity at  $P$  equal to

$$\mathbf{dV} = \frac{\Gamma}{4\pi} \frac{d\mathbf{l} \times \mathbf{r}}{|\mathbf{r}|^3} \quad (5.5)$$

Equation (5.5) is called the ***Biot-Savart law*** and is one of the most fundamental relations in the theory of inviscid, incompressible flow.

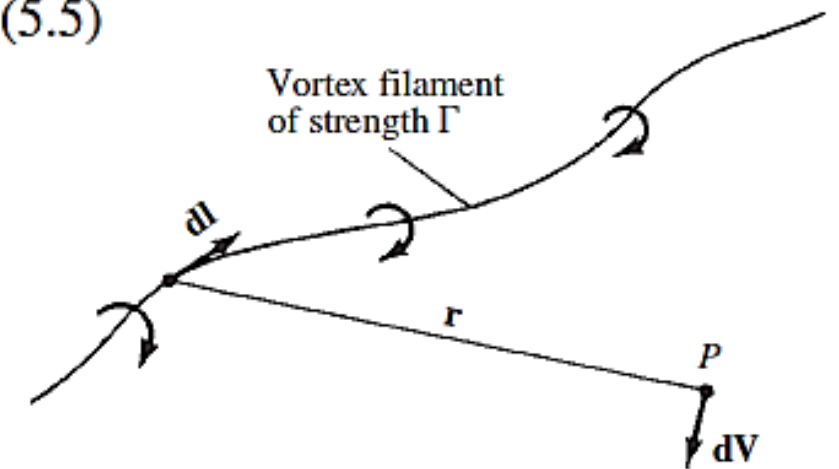


**Figure 5.8** Vortex filament and illustration of the Biot-Savart law.



# THE VORTEX FILAMENT, THE BIOT-SAVART LAW

Apply the Biot-Savart law to a straight vortex filament of infinite length, as sketched in Figure 5.9. The strength of the filament is  $\Gamma$ . The velocity induced at point  $P$  by the directed segment of the vortex filament  $d\mathbf{l}$  is given by Equation (5.5). Hence, the velocity induced at  $P$  by the entire vortex filament is

$$\mathbf{V} = \int_{-\infty}^{\infty} \frac{\Gamma}{4\pi} \frac{d\mathbf{l} \times \mathbf{r}}{|\mathbf{r}|^3} \quad (5.7)$$

From the definition of the vector cross product (see Section 2.2), the direction of  $\mathbf{V}$  is downward in Figure 5.9. The magnitude of the velocity,  $V = |\mathbf{V}|$ , is given by

$$V = \frac{\Gamma}{4\pi} \int_{-\infty}^{\infty} \frac{\sin \theta}{r^2} dl \quad (5.8)$$

In Figure 5.9, let  $h$  be the perpendicular distance from point  $P$  to the vortex filament. Then, from the geometry shown in Figure 5.9,

$$r = \frac{h}{\sin \theta} \quad (5.9a)$$

$$l = \frac{h}{\tan \theta} \quad (5.9b)$$

$$dl = -\frac{h}{\sin^2 \theta} d\theta \quad (5.9c)$$

Equation (5.9a to c) in Equation (5.8), we have

$$V = \frac{\Gamma}{4\pi} \int_{-\infty}^{\infty} \frac{\sin \theta}{r^2} dl = -\frac{\Gamma}{4\pi h} \int_{\pi}^0 \sin \theta d\theta$$

$$V = \frac{\Gamma}{2\pi h} \quad (5.10)$$

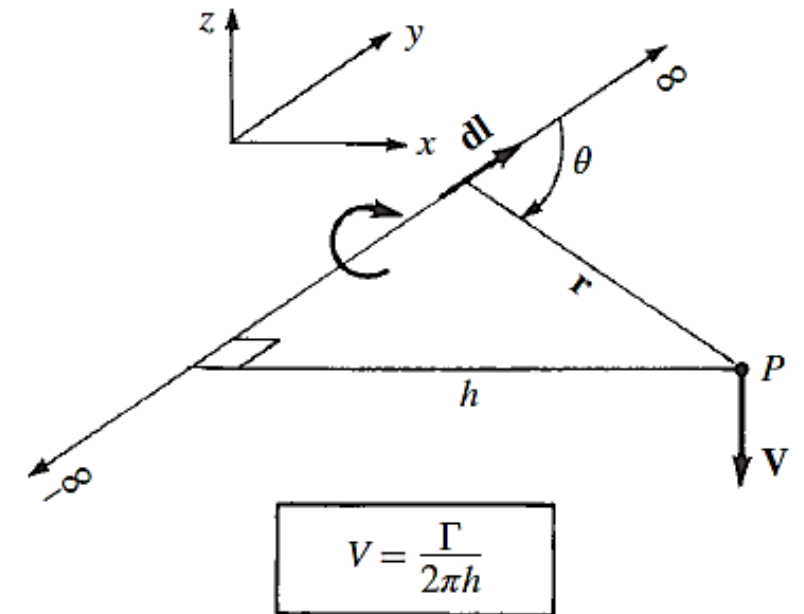


**Figure 5.9** Velocity induced at point  $P$  by an infinite, straight vortex filament.

Induced velocity is found as same as a point vortex in two-dimensional flow.



# THE VORTEX FILAMENT, THE BIOT-SAVART LAW

Consider the *semi*-infinite vortex filament shown in Figure 5.10. The filament extends from point  $A$  to  $\infty$ . Point  $A$  can be considered a boundary of the flow. Let  $P$  be a point in the plane through  $A$  perpendicular to the filament. Then, by an integration similar to that above (try it yourself), the velocity induced at  $P$  by the semi-infinite vortex filament is

$$V = \frac{\Gamma}{4\pi h} \quad (5.11)$$

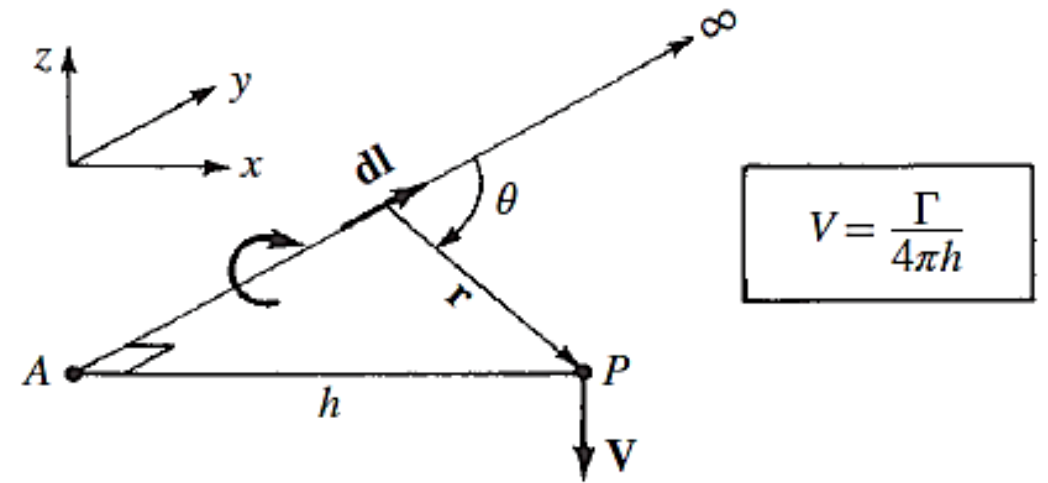


**Figure 5.10** Velocity induced at point  $P$  by a semi-infinite straight vortex filament.



# PRANDTL'S CLASSICAL LIFTING-LINE THEORY

Prandtl reasoned as follows. A vortex filament of strength  $\Gamma$  that is somehow bound to a fixed location in a flow - a so-called bound vortex- will experience a force  $L' = \rho_\infty V_\infty \Gamma$  from the Kutta-Joukowski theorem. This bound vortex is in contrast to a *free vortex*, which moves with the same fluid elements throughout a flow. Therefore, let us replace a finite wing of span  $b$  with a bound vortex, extending from  $y = -b/2$  to  $y = b/2$ , as sketched in Figure 5.12. However, due to Helmholtz's theorem, a vortex filament cannot end in the fluid. Therefore, assume the vortex filament continues as two free vortices trailing downstream from the wing tips to infinity, as also shown in Figure 5.12. This vortex (the bound plus the two free) is in the shape of a horseshoe, and therefore is called a **horseshoe vortex**.

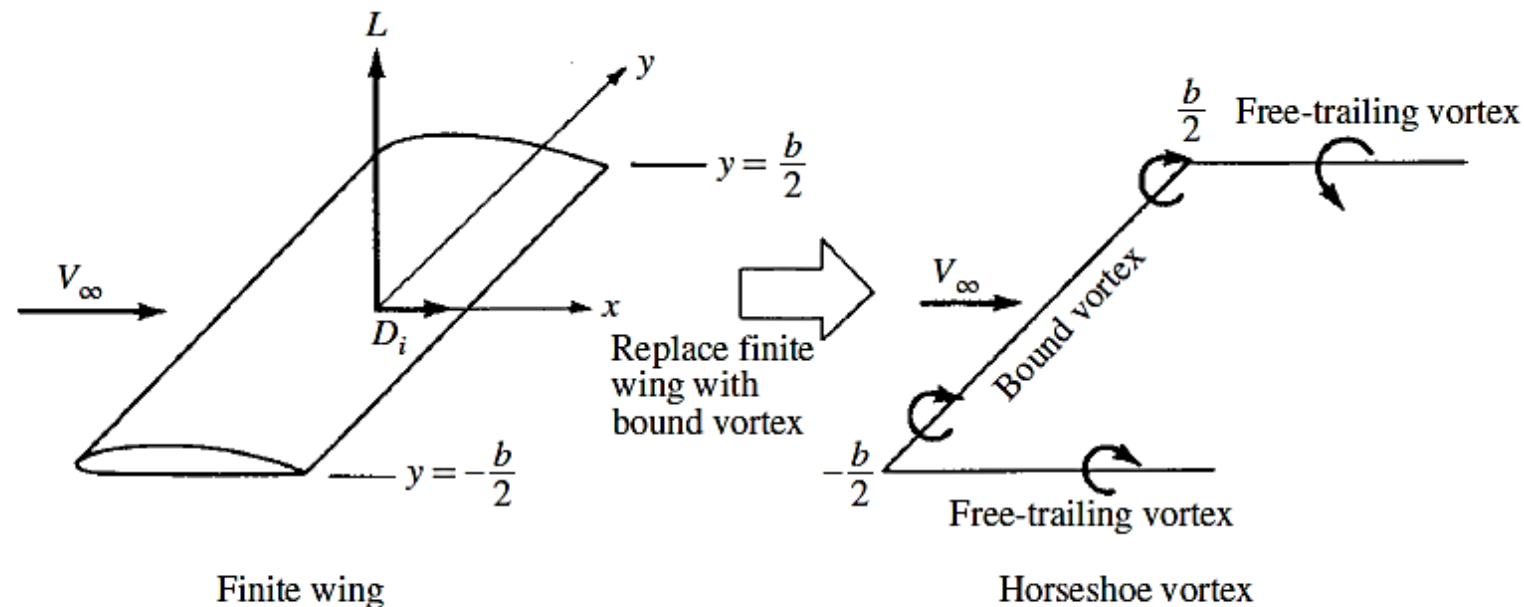


**Figure 5.12** Replacement of the finite wing with a bound vortex.





# PRANDTL'S CLASSICAL LIFTING-LINE THEORY

$$dw = -\frac{(d\Gamma/dy) dy}{4\pi(y_0 - y)} \quad (5.14)$$

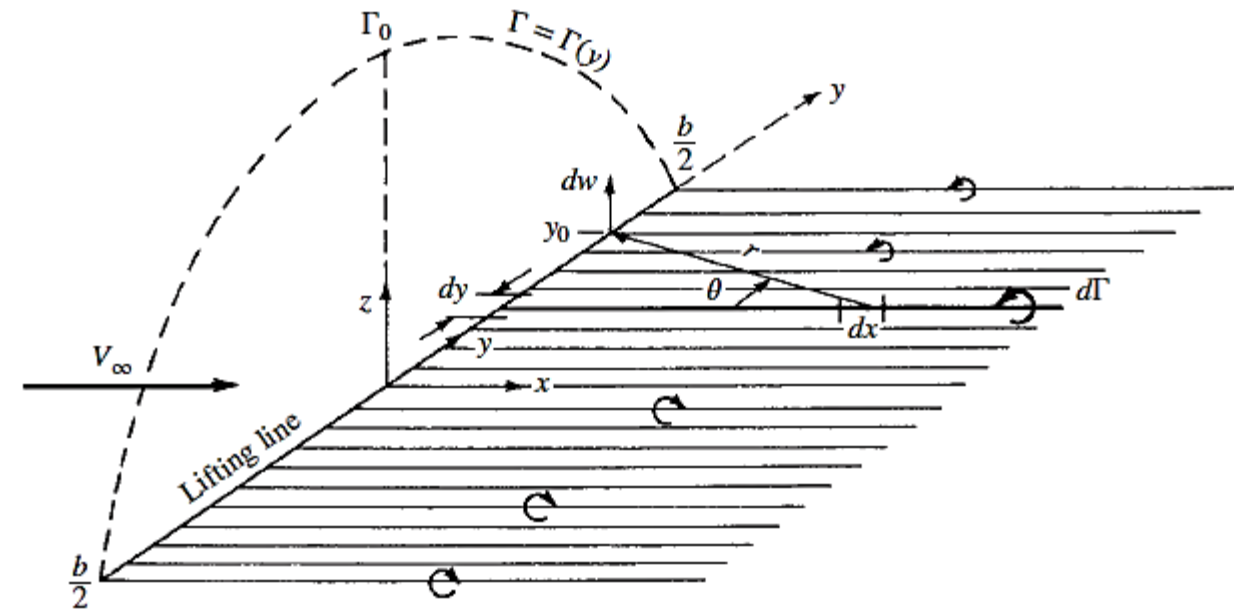


**Figure 5.15** Superposition of an infinite number of horseshoe vortices along the lifting line.

The total velocity  $w$  induced at  $y_0$  by the entire trailing vortex sheet is the summation of Equation (5.14) over all the vortex filaments, that is, the integral of Equation (5.14) from  $-b/2$  to  $b/2$ :

$$w(y_0) = -\frac{1}{4\pi} \int_{-b/2}^{b/2} \frac{(d\Gamma/dy) dy}{y_0 - y} \quad (5.15)$$



# PRANDTL'S CLASSICAL LIFTING-LINE THEORY

$$\alpha(y_0) = \frac{\Gamma(y_0)}{\pi V_\infty c(y_0)} + \alpha_{L=0}(y_0) + \frac{1}{4\pi V_\infty} \int_{-b/2}^{b/2} \frac{(d\Gamma/dy) dy}{y_0 - y} \quad (5.23)$$

the *fundamental equation of Prandtl's lifting-line theory*; it simply states that the geometric angle of attack is equal to the sum of the effective angle plus the induced angle of attack. In Equation (5.23),  $\alpha_{\text{eff}}$  is expressed in terms of  $\Gamma$ , and  $\alpha_i$  is expressed in terms of an integral containing  $d\Gamma/dy$ . Hence, Equation (5.23) is an integro-differential equation, in which the only unknown is  $\Gamma$ ; all the other quantities,  $\alpha$ ,  $c$ ,  $V_\infty$ , and  $\alpha_{L=0}$ , are known for a finite wing of given design at a given geometric angle of attack in a freestream with given velocity. Thus, a solution of Equation (5.23) yields  $\Gamma = \Gamma(y_0)$ , where  $y_0$  ranges along the span from  $-b/2$  to  $b/2$ .



# PRANDTL'S CLASSICAL LIFTING-LINE THEORY

## 5.3.1 Elliptical Lift Distribution

Consider a circulation distribution given by

$$\Gamma(y) = \Gamma_0 \sqrt{1 - \left(\frac{2y}{b}\right)^2} \quad (5.31)$$

$$\alpha_i = \frac{C_L}{\pi AR} \quad (5.42a)$$

$$AR \equiv \frac{b^2}{S}$$

Equation (5.42a) is a useful expression for the induced angle of attack, as shown below.

$$C_{D,i} = \frac{C_L^2}{\pi AR} \quad (5.43)$$



## Lift curve for infinite and finite wing

The typical lift curve for a three-dimensional wing composed of a given airfoil section is compared in Fig. 5.26 with that for a two-dimensional airfoil having the same airfoil section. Notice that the lift-curve slope for the three-dimensional wing (which is represented by the symbol  $C_{L_\alpha}$ ) is considerably less than the lift-curve slope for an unswept, two-dimensional airfoil (which is represented by the symbol  $C_{l_\alpha}$ ). Recall that a lift-curve slope of approximately 0.1097 per degree is typical for an unswept two-dimensional airfoil, as discussed in Section 5.4.1. As we will find out in Chapter 7, the lift-curve slope for an ideal three-dimensional unswept wing ( $C_{L_\alpha}$ ) is:

$$C_{L_\alpha} = a = \frac{C_{l_\alpha}}{1 + \frac{C_{l_\alpha}}{\pi AR}} = \frac{a_0}{1 + \frac{a_0}{\pi AR}} \quad (5.41)$$

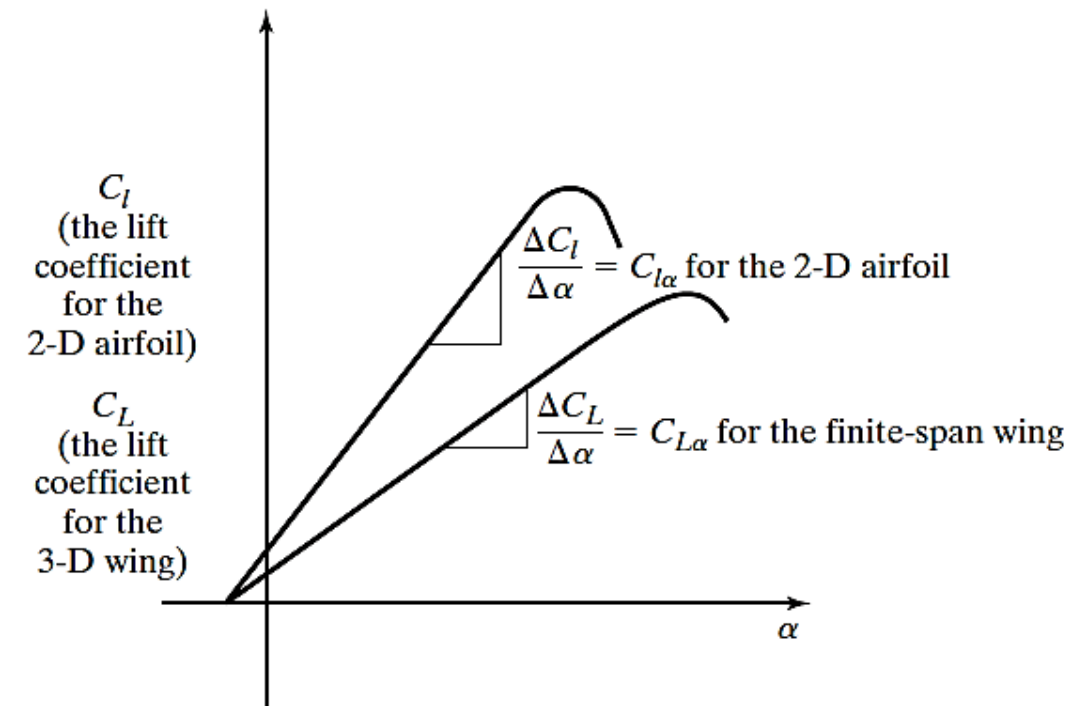


**Figure 5.26** Comparison of the lift-curve slope of a two-dimensional airfoil with that for a finite-span wing.